CHAPTER 3: Optical Filters

In This Chapter...

3.1 Introduction

A set of 48 filters are included in WFPC2 with the following features:

1. It approximately replicates the WF/PC-1 "UBVRI" photometry series.
2. The broad-band filter series extends into the far UV.
3. There is a Strömgren series.
4. A Wood's filter is available for far-UV imaging without a red leak.
5. There is a 1% bandpass linear ramp filter series covering 3700-9800Å.
6. The narrow-band series is uniformly specified and well calibrated.

The filters are mounted in the Selectable Optical Filter Assembly (SOFA) between the shutter and the reflecting pyramid. The SOFA contains 12 filter wheels, each of which has 4 filters and a clear "home" position. A listing of all simple optical elements in the SOFA mechanism, and the location of each element (by wheel number 1-12, and position 1-4) is given in Table 3.1. Wheel number 1 is located closest to the shutter. The categories of simple filters (F) are long-pass (LP), wide (W), medium (M), and narrow (N). Most of these filters are either flat single substrates or sandwiches.

The filter complement includes two solar blind Wood's filters, F160AW and F160BW. F160BW is used in all science observations because the other filter has some large pinholes that lead to significant red leak.

In addition to the above complement of broad and narrow-band filters, WFPC2 features a set of three specialized quadrant (quad or Q) filters in which each quadrant corresponds to a facet of the pyramid, and therefore to a distinct camera relay. There is one quad containing four narrow-band, redshifted [OII] filters with central wavelengths from 3763Å to 3986Å, one quad with four polarizing elements (POL) with polarization angles, 0°, 45°, 90° and 135°, and one quad with four methane (CH4) band filters with central wavelengths from 5433Å to 8929Å. The polarizer quad filter can be crossed with any other filter over the wavelength range from 2800Å to 8000Å, with the exception of the Methane Quad and Redshifted [OII] Quad which share the same wheel. The SOFA also contains four linearly variable narrow-band ramp (FR) filters (in the twelfth wheel - closest to the focus). The quad and ramp filters are listed in Table 3.2.

In Table 3.1 and Table 3.2, each of the type "A" filters is equivalent to inserting 5 mm of quartz in terms of optical path length, with compensation for wavelength such that focus is maintained on the CCDs. A configuration with no filters in the beam results in out-of-focus images and generally will not be used. With the exception of the quad polarizer and blocking (Type "B") filters, all filters are designed to be used alone. Type "B" filters introduce no focus shift, so they can be used in combination with any type "A" filter. All combinations where the number of type "A" filters is not unity will result in out-of-focus images. The image blur resulting from two or zero type "A" filters at visible wavelengths is equivalent to 2.3 mm defocus in the F/24 beam, which corresponds to 1/5 wave RMS of defocus at 6328Å, and a geometrical image blur of 0.34″. While this is a large defocus, the images are still of very high quality compared to seeing limited images. Some such combinations may be scientifically attractive. For example, the Wood's filter may be crossed with another UV filter to provide a solar blind passband (although the efficiency will be low).

The mean wavelength, $\bar{\lambda}$, is similar to that defined in Schneider, Gunn and Hoessel (Ap. J. 264, 337). The width is the FWHM of a Gaussian filter with the same second moment, and is reasonably close to the FWHM. The values tabulated here do not include the CCD DQE or the transmission of the OTA or WFPC2 optics (as given in Figure 2.4). In Chapter 6, the corresponding quantities are given including the effect of the other optical elements and the CCD DQE.

Figure 3.1 summarizes the normalized transmission curves for the simple filters and narrow-band quad filters. It does not include curves for the polarizing quad, or the linear ramp filters which are documented in sections 3.2 and 3.4 respectively. Individual filter transmission curves are shown in the Appendix starting on page 201. Figure 3.1 divides the filters into the following groups:

1. Long pass filters designed to be used in combination with another filter.
2. Wide bandpass filters with FWHM ~25% of the central wavelength.
3. Approximations to the UBVRI sequence, generally with wider bandpasses, designed for use on faint sources.
4. A photometric set of approximations to UBVRI passbands (see Harris et al. 1991, A.J. 101, 677). Note, however, that the WFPC2 UBVRI series is not the Johnson-Cousins photometric series, neither is it identical with the WF/PC-1 series. See Chapter 6 for detailed comparisons.

Table 3.1: WFPC2 Simple Filter Set. The effective wavelength, width, and transmission quoted are defined precisely in Chapter 6, but here are quoted without the system (OTA_WFPC2) response.

Name	Type	Wheel	Slot	Notes	In WF/PC-1?	$\bar{\lambda}$(Å)	$\Delta\bar{\lambda}$(Å)	Peak T (%)	Peak λ (Å)
F122M	A	1	4	H Ly α - Red Leak	Y	1292	263.5	18.9	1240
F130LP	B	2	1	CaF2 Blocker (zero focus)	N	3847	5568.1	94.7	4344
F160AW	A	1	3	Woods A - redleak from pinholes	N	1471	457.2	10.1	1403
F160BW	A	1	2	Woods B	N	1471	457.2	10.1	1403
F165LP	B	2	2	Suprasil Blocker (zero focus)	N	4327	5505.7	92.1	3109
F170W	A	8	1	-	N	1689	434.9	30.3	1667
F185W	A	8	2	-	N	1907	302.9	23.7	1849
F218W	A	8	3	Interstellar feature	N	2136	355.9	21.3	2091
F255W	A	8	4	-	N	2557	408.2	15.5	2483
F300W	A	9	4	Wide U	N	2924	727.6	51.8	2760
F336W	A	3	1	WFPC2 U, Strömgren *u*	Y	3327	370.7	80.3	3447
F343N	A	5	1	Ne V	N	3430	24.3	19.7	3433
F375N	A	5	2	[OII] 3727 RS	Y	3736	26.2	17.2	3736
F380W	A	9	1	-	N	3934	694.7	65.6	3981
F390N	A	5	3	CN	N	3889	45.3	37.8	3886
F410M	A	3	2	Strömgren *v*	N	4088	146.9	70.1	4098
F437N	A	5	4	[OIII]	Y	4369	25.2	52.0	4368
F439W	A	4	4	WFPC2 B	Y	4292	464.4	67.3	4176
F450W	A	10	4	Wide B	N	4445	925.0	92.4	5061
F467M	A	3	3	Strömgren *b*	N	4682	171.5	75.3	4728
F469N	A	6	1	He II	Y	4695	24.9	52.4	4699
F487N	A	6	2	H β	Y	4865	25.8	58.6	4863
F502N	A	6	3	[OIII]	Y	5012	26.8	63.8	5009
F547M	A	3	4	Strömgren *y* (but wider)	Y	5454	486.6	91.3	5361
F555W	A	9	2	WFPC2 V	Y	5252	1222.5	94.8	5151
F569W	A	4	2	F555W generally preferred[a]	Y	5554	965.8	94.2	5309
F588N	A	6	4	He I & Na I (NaD)	Y	5892	49.1	91.5	5895
F606W	A	10	2	Wide V	Y	5843	1578.7	98.3	6183
F622W	A	9	3	-	Y	6157	935.4	95.6	6034
F631N	A	7	1	[OI]	Y	6306	30.8	85.7	6302
F656N	A	7	2	Hα	Y	6562	22.0	77.9	6561
F658N	A	7	3	[NII]	Y	6590	28.5	79.7	6592
F673N	A	7	4	[SII]	Y	6733	47.2	87.0	6733
F675W	A	4	3	WFPC2 R	Y	6735	889.4	97.9	6796
F702W	A	10	3	Wide R	Y	6997	1480.7	98.5	6539
F785LP	A	2	3	F814W generally preferred[a]	Y	9366	2094.7	96.0	9960
F791W	A	4	1	F814W generally preferred[a]	Y	8006	1304.2	99.7	8081
F814W	A	10	1	WFPC2 I	Y	8269	1758.0	98.4	8386
F850LP	A	2	4	-	Y	9703	1669.5	95.5	10026
F953N	A	1	1	[SIII]	N	9546	52.5	95.6	9528
F1042M	A	11	2	-	Y	10443	610.9	95.2	10139

a. Filters F555W and F814W are generally preferred, as they are part of the “standard” WFPC2 filter set, and will tend to have slightly better photometric calibration. See “Choice of Broad Band Filters” on page 40.

Table 3.2: WFPC2 Quad and Ramp Filters. Segments of the UV and CH4 quads are labeled here by their usual physical designations (A, B, C, and D); see following sections for filter and aperture names which are to be used in writing Phase II proposal. The quad polarizer is represented for both parallel and perpendicular polarization to its polarization direction, which is different in each quadrant.

Physical Name	Type	Wheel	Slot	Notes	In WF/PC-1	$\bar{\lambda}$(Å)	$\Delta\bar{\lambda}$(Å)	Peak T (%)	Peak λ (Å)
FQUVN-A	A	11	3	Redshifted [OII] 375	N	3767	73.4	24.0	3769
FQUVN-B	A	11	3	Redshifted [OII] 383	N	3831	57.4	30.5	3827
FQUVN-C	A	11	3	Redshifted [OII] 391	N	3915	59.3	38.9	3908
FQUVN-D	A	11	3	Redshifted [OII] 399	N	3993	63.6	43.4	3990
FQCH4N-A	A	11	4	CH4 543	N	5433	38.0	83.8	5442
FQCH4N-B	A	11	4	CH4 619	N	6193	44.0	83.7	6202
FQCH4N-C	A	11	4	CH4 727	N	7274	51.0	89.7	7279
FQCH4N-D	A	11	4	CH4 892	N	8929	64.0	91.2	8930
POLQ_par	B	11	1	Pol angle 0˚,45˚,90˚,135˚	N	5427	5797.6	90.8	10992
POLQ_per	B	11	1	Pol angle 0˚,45˚,90˚,135˚	N	7922	6653.4	89.7	10992
FR418N	A	12	1	3700-4720	N	W	W/75	~20-50	W
FR533N	A	12	2	4720-6022	N	W	W/75	~40-50	W
FR680N	A	12	3	6022-7683	N	W	W/75	~60-80	W
FR868N	A	12	4	7683-9802	N	W	W/75	~70-85	W

5. Medium bandpass filters with FWHM ~10% of the central wavelength, including an approximation to the Strömgren photometric series.
6. Narrow bandpass filters for isolating individual spectral lines or bands.
7. Redshifted [OII] and CH4 narrow bandpass quad filters.

Note that the UV filters have some degree of "red leak," which is quantified in Chapter 6 where the system response is included.

A passband calibration is maintained in the calibration database system (CDBS). It has been updated following on orbit calibrations. The ground based calibration of the narrow-band filters' central wavelengths has not been corrected for temperature effects and is therefore accurate to about 2Å. Because of this, it is not advisable to place narrow emission lines at the half power points of such filters and expect to predict the throughput to high accuracy. The standalone software package XCAL, or SYNPHOT running under IRAF, can be used to access these calibrations which are available on the Institute's WWW page.

Figure 3.1: Summary of Normalized Filter Curves.

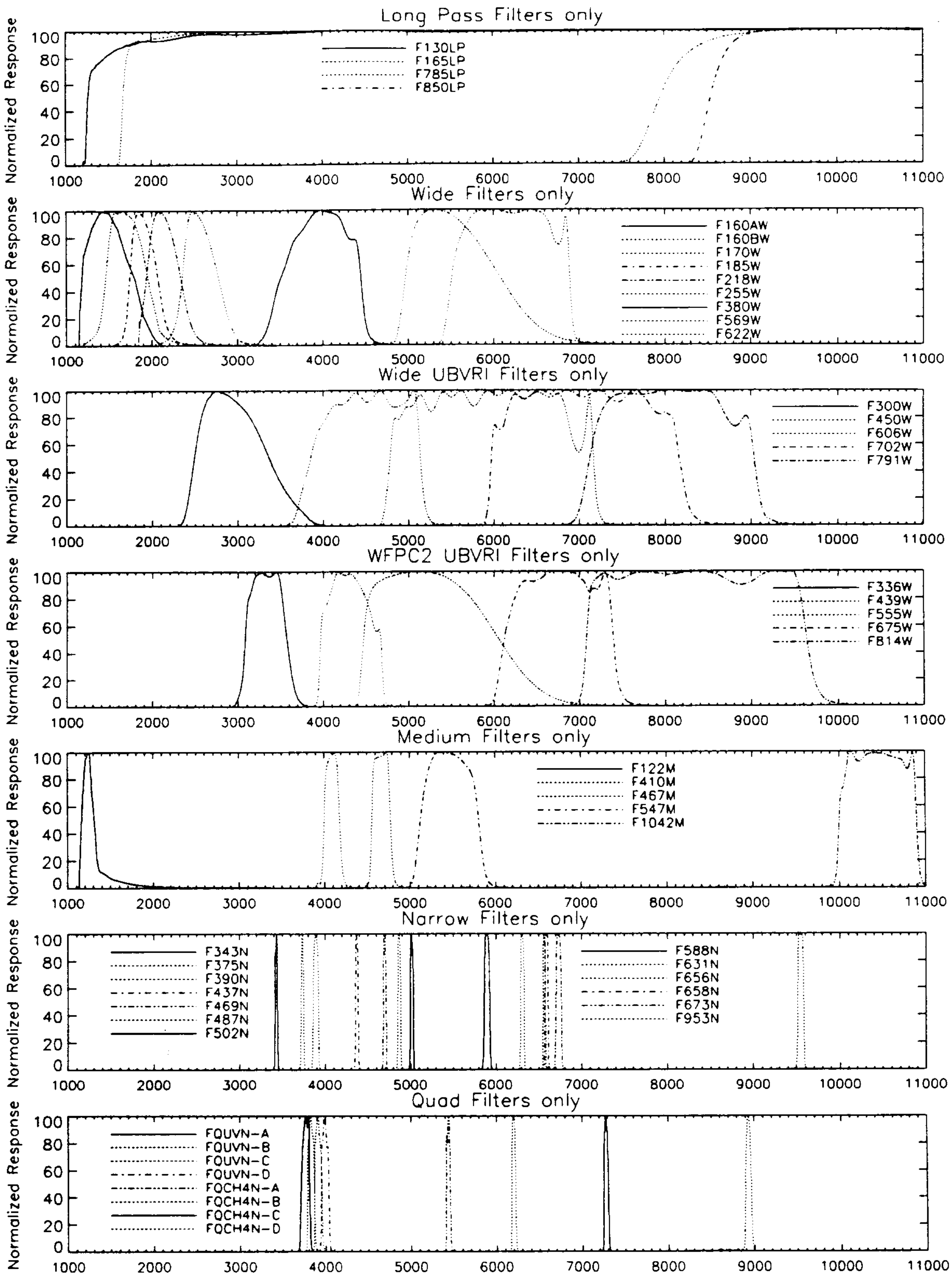

3.2 Choice of Broad Band Filters

A number of different choices are possible on WFPC2 in order to approximate the Johnson-Cousins system often used in ground based observing. These choices differ in throughput, wavelength fidelity, color transformability, and cosmetics. The HST science program as a whole benefits if a standard set can be agreed upon by the community for broad band photometry. This will allow theoretical isochrones and other models to be published in the standard system, and allow ready comparison of the results from different observers. Furthermore, although all filters will be calibrated photometrically and with flat fields, a core set must be chosen for monitoring the instrument both photometrically and in imaging performance. There was a substantial consensus between the accepted Cycle 4 GO programs and the WF/PC-1 and WFPC2 science teams that F336W, F439W, F555W, F675W, and F814W should be the preferred set to approximate the Johnson Cousins U, B, V, R, I passbands. These filters form the basis for the WFPC2 broad band photometric system. As will be seen from the figures in Section 8.8 (page 172), the preferred set is accurately transformable with the exception of the U bandpass.

On the other hand, there are situations where concerns such as maximum throughput must override the above arguments. For example, filters F300W, F450W, F606W, and F814W were chosen for the Hubble Deep Field (HDF), due to their wider bandpasses.

3.3 Linear Ramp Filters

The linear ramp filters are designed for narrow-band absorption and emission line imaging of moderately extended objects. Each filter is divided into four parallel strips where the central wavelength across each strip varies by approximately 6%. Each CCD pixel is mapped to a unique central wavelength with a FWHM bandwidth of approximately 1.3% of the central wavelength. The maximum size of an object which can be imaged at a given wavelength is approximately 13″ and is determined by the width of the strips and the image size at the filter. The cumulative wavelength range of the four linear ramp filters is 3710Å to 9762Å. Originally intended for a four WFC configuration, the linear ramp filters require partial rotation of the SOFA wheels to +15°, -18° and -33° from their nominal positions, to recover wavelength regions which would fall on the PC camera or otherwise be lost. There will be vignetting at some wavelengths for these partial rotations.

3.3.1 Spectral Response

A JPL Memorandum (DFM #2031, 1992) gives the results of a prediction scheme to locate and quantify the passbands of the four WFPC2 ramp filters, FR418N, FR533N, FR680N and FR866N. The results are summarized here.

Laboratory (room temperature) measurements of the passbands of the four ramp filters were made at five equally spaced intervals on each of the four ramp stripes on each filter for a total of 80 passband measurements. The laboratory measurements were made with a narrow beam and were then integrated over an annular area of the filter to simulate the beam profile. The radius of the beam is 3.7 mm, or 13″. The integration was carried out by assuming the nominal linear shift in wavelength with position, and that no significant changes in the passband shape occur across the beam. The integration makes the shape of the passband quite symmetrical.

The resulting spectral response can be fitted to within a few percent with a Munson function:

$$T = T_0 / \{1 + (1-a)x^2 + a(1-b)x^4 + ab(1-c)x^6 + abcx^8\}$$

where a, b and c are shape parameters, and $0 \le (a,b,c) \le 1$; T_0 is the peak transmission of the passband, $T=T_0$ at $x=0$; x is related to wavelength λ by $x=(\lambda-\lambda_0)/H$, $T=T_0/2$ at $x=1$ (so H is the half width at half maximum).

The parameters, (λ_0, T_0, H, a, b, c) were then fitted to polynomial functions of position Y (which starts at 0 inches at the lower wavelength edge of each strip) to predict the filter response for areas of the filters between the tested points. Good quadratic fits are available for all the parameters except for T_0 which requires a cubic. The results are given in Tables 3.3 through 3.6, which give the polynomial fit coefficients for the ramp filter parameters. The table entries, except for the first line, are used as parameter$=A_0+A_1Y+A_2Y_2+A_3Y_3$. The short wavelength side of the filter is opposite for alternate ramps. The first line in each table gives the Y position as a function of λ. If the polynomial fit predicts a, b, or $c < 0$ or > 1 then the quantities are set to 0 or 1 respectively.

Use of these fits should be restricted to objects near the center of the ramp, otherwise the beam will combine light from adjacent ramps. The fit should also not be used within 13″ of the end of the ramp. There is enough wavelength overlap between ramps that the extreme ends need not be used, except at the very lowest and highest wavelengths. Figure 3.2 shows the fit parameter T_0 as a function of λ_0 for all 16 ramp filter strips. Figure 3.3 shows $2H/\lambda_0$.

Figure 3.2: Ramp Filter Peak Transmission. The four line types correspond to the four different filters (each containing four ramps).

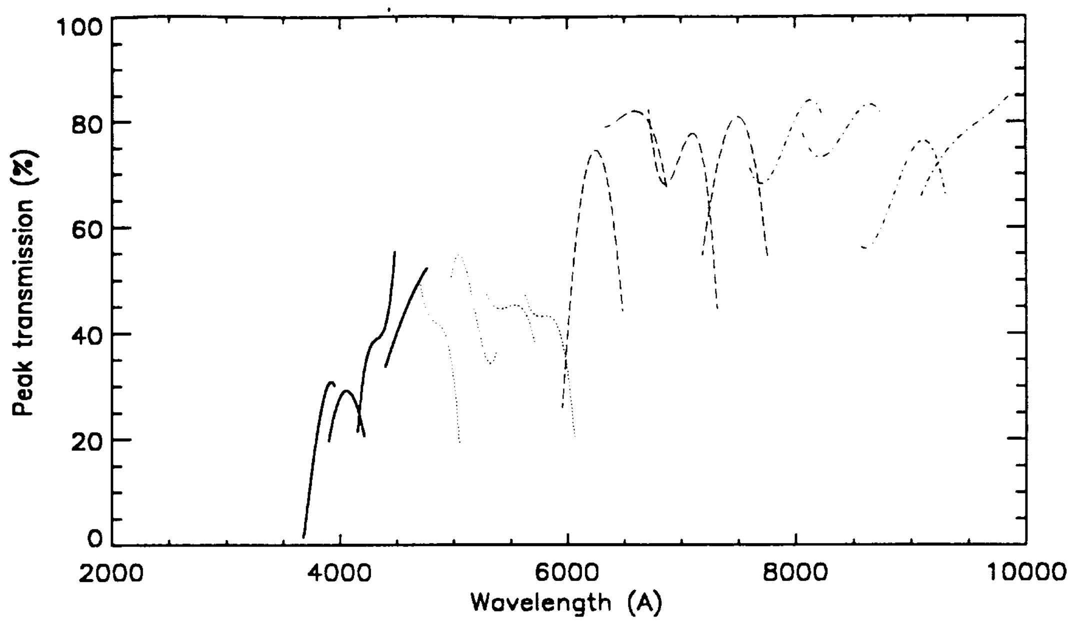

Figure 3.3: Ramp Filter Dimensionless Widths.

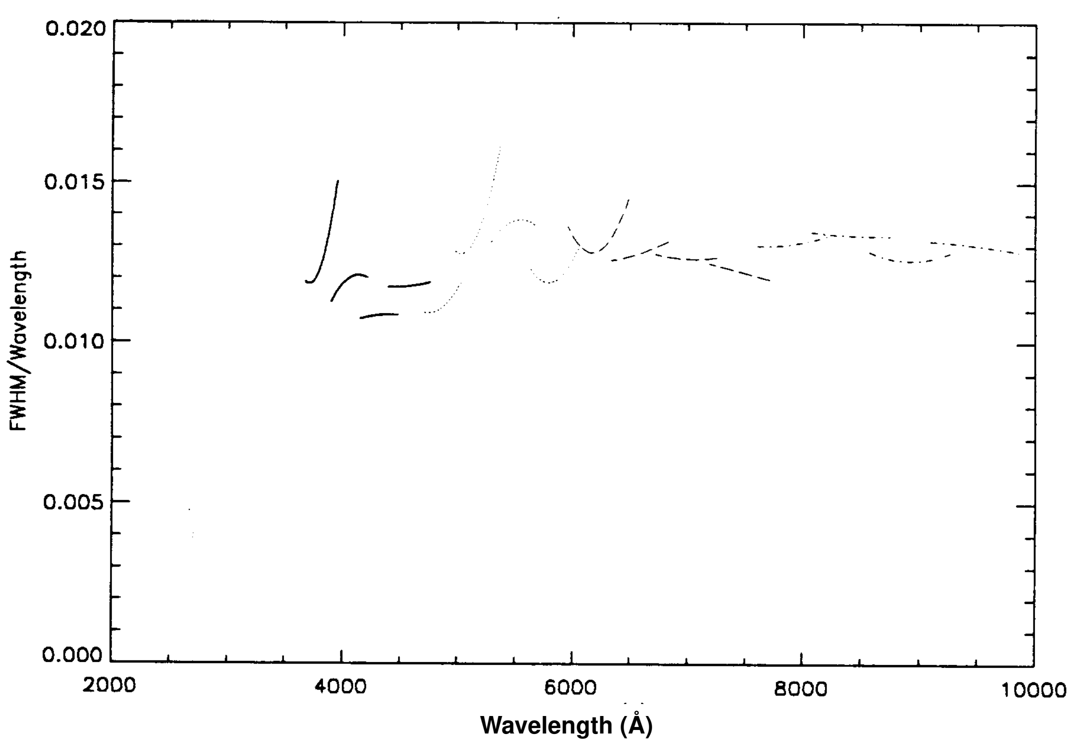

Table 3.3: Ramp Filter FR418N Parameters.

Quantity	A0	A1	A2	A3
Ramp 1 Position	-26.1083	.00713888	.0000	
Wavelength	3657.7	138.7	.6178	
Peak transmission	-.01667	.2188	.04138	-.03489
Half width at half max	21.95	-.8347	2.143	
a	.2120	.002857	.002596	
b	1.181	-.8138	.3535	
c	.3301	-.3715	.3825	
Ramp 2 Position	-24.2554	.00625704	.0000	
Wavelength	3876.9	158.6	.5472	
Peak transmission	.1660	.2288	-.1080	.004005
Half width at half max	21.50	3.315	-.7079	
a	.1592	-.003687	-.0008497	
b	.7938	.2355	-.09124	
c	.9306	.01366	.007458	
Ramp 3 Position	-24.7145	.00598254	.0000	
Wavelength	4130.5	168.8	-.7389	
Peak transmission	.1352	.6200	-.5226	.1529
Half width at half max	22.09	1.306	-.1181	
a	.2300	.05586	-.03044	
b	1.096	-.3185	.1396	
c	1.276	-1.279	.5721	
Ramp 4 Position	-23.4440	.00536340	.0000	
Wavelength	4371.3	185.8	.2913	
Peak transmission	.3189	.1287	-.01160	-.001712
Half width at half max	25.62	1.015	.1161	
a	.3123	-.2055	.09535	
b	.9222	.1167	-.04673	
c	1.033	-.1356	.05660	

Table 3.4: Ramp Filter FR533N Parameters.

Quantity	A0	A1	A2	A3
Ramp 1 Position	-26.7670	.00572115	.0000	
Wavelength	4677.7	177.3	-1.125	
Peak transmission	.5450	-.3612	.3623	-.1281
Half width at half max	25.67	.3168	.8873	
a	-.009839	.4644	-.2039	
b	.31511	.9473	-.4516	
c	-.3379	2.788	-1.346	
Ramp 2 Position	-24.6600	.00498393	.0000	
Wavelength	4948.4	199.2	.6484	
Peak transmission	.4546	.4188	-.5456	0.1548
Half width at half max	32.10	-1.204	3.171	
a	.1678	-.02726	.09521	
b	.9345	.1935	-.1224	
c	.9571	.02919	-.009393	
Ramp 3 Position	-24.5038	.00465985	.0000	
Wavelength	5257.3	217.9	-1.481	
Peak transmission	.4944	-.1714	.1890	-0.0631
Half width at half max	34.03	5.078	-1.347	
a	.3851	-.06264	.003163	
b	.5605	.6642	-.2751	
c	.9665	.05543	-.03654	
Ramp 4 Position	-25.5182	.00455886	.0000	
Wavelength	5596.9	220.9	-.6938	
Peak transmission	.5058	-.2715	.3203	-.1230
Half width at half max	35.06	-2.856	2.382	
a	.06553	.2253	-.08275	
b	1.043	-.1190	.02889	
c	1.162	-.4910	.2059	

Table 3.5: Ramp Filter FR680N Parameters.

Quantity	A0	A1	A2	A3
Ramp 1 Position	-21.8962	.00370137	.0000	
Wavelength	5916.0	269.4	.3460	
Peak transmission	.1198	1.005	-.4015	-.00162
Half width at half max	41.50	-5.873	4.038	
a	.1743	-.05050	.06481	
b	.8320	.3326	-.1858	
c	.9682	-.09110	.05122	
Ramp 2 Position	-22.6919	.00360750	.0000	
Wavelength	6290.8	275.6	.7184	
Peak transmission	.7918	-.02034	.1086	-.05945
Half width at half max	39.48	2.120	.3703	
a	.05596	.3034	-.1333	
b	1.017	-.27026	.04560	
c	.7244	.8326	-.5107	
Ramp 3 Position	-22.0719	.00330755	.0000	
Wavelength	6673.5	301.6	.3321	
Peak transmission	.9494	-1.008	1.161	-.3777
Half width at half max	42.81	.8193	.4269	
a	.1038	.09020	-.02747	
b	.8415	.3045	-.1930	
c	1.017	-.1732	.07463	
Ramp 4 Position	-24.7447	.00346462	.0000	
Wavelength	7141.9	289.3	-.2999	
Peak transmission	.4823	.4479	-.07484	-.05868
Half width at half max	44.72	.8952	-.0756	
a	.1612	-.01167	.01355	
b	.2708	1.077	-.4757	
c	.9941	-.02694	.01685	

Table 3.6: Ramp Filter FR868N Parameters.

Quantity	A0	A1	A2	A3
Ramp 1 Position	-23.2685	.00308029	.0000	
Wavelength	7555.5	320.4	1.906	
Peak transmission	.7524	-.3328	.4543	-.1343
Half width at half max	49.32	1.742	.4914	
a	.2958	-.3877	.2465	
b	1.321	-.9156	.3666	
c	.3762	1.668	-.9499	
Ramp 2 Position	-22.9766	.00286673	.0000	
Wavelength	8014.3	350.5	-.7500	
Peak transmission	.8204	-.3368	.3815	-.1057
Half width at half max	54.17	1.579	.2196	
a	.05832	.7525	-.3625	
b	.4582	.8433	-.4350	
c	.6422	.3247	-.1593	
Ramp 3 Position	-22.6085	.00265657	.0000	
Wavelength	8510.7	375.6	.3706	
Peak transmission	.5817	-.1920	.4517	-.1627
Half width at half max	55.19	-.7459	1.433	
a	.5422	-.2444	.03545	
b	1.420	-1.176	.4814	
c	.4257	-.2522	.1777	
Ramp 4 Position	-23.2142	.00256976	.0000	
Wavelength	9034.3	387.2	.8722	
Peak transmission	.6241	.2403	-.1230	.02829
Half width at half max	59.69	2.167	-.1996	
a	.2376	-.01879	-.00864	
b	.9670	.02456	-.00477	
c	.7829	.03750	.02393	

3.3.2 Target Locations

In Figures 3.4 and 3.5 we show the correspondence between central wavelength and location in the focal plane for the nominal and rotated filter positions. The selection of filter and aperture for the linear ramp filters is transparent to the user who is required only to specify the linear ramp filter name LRF and a central wavelength. Each central wavelength is assigned to a unique filter and CCD location.

Following on-orbit testing of WFPC2 a revised table of linear ramp filter wavelengths has been compiled and is shown in Table 3.7. For each wavelength listed, there is a minimum 10″ diameter unvignetted field-of-view. Some wavelengths can be obtained with several different settings of the ramps, however, for simplicity, the redundant wavelengths have been removed from the table. Note that this table supports observation with the PC and a new $+15^{\circ}$ rotation of the filter wheel. Table 3.8 lists wavelengths which are available, but with some compromise in data quality, so as to avoid gaps in wavelength coverage. Most of these wavelengths are observed slightly off the central wavelength of the passband. This implies a slightly reduced throughput (see estimates of the light reduction in the table), and some additional difficulties in flattening the data to remove variations in the passband across the target. A few other wavelengths are observed slightly off the unvignetted centerline of the ramps, and these are indicated by note “FOV” in Table 3.8. Again, this vignetting will present some additional complications when calibrating the data. Further details regarding the ramp filter wavelengths and apertures will be made available in a separate instrument science report.

We note that an interactive tool is available on the WFPC2 WWW pages which will compute target locations for LRF observations. The user inputs either the central wavelength or the target location in the field-of-view, and the other quantity is returned.

3.3.3 LRF Photometric Calibration

As of this writing, the preferred method of flat fielding LRF data is to use a narrow band flat observed nearby in wavelength. This will remove pixel-to-pixel effects, as well as effects of distortion and vignetting in the cameras, while avoiding the complications of pinholes on the LRFs and spurious variations due to the spectrum of the flat field light source.

Conversion of counts to source flux is best achieved by using the SYNPHOT synthetic photometry package. An LRF filter setting is simply specified by including “LRF#*xxxx*” in the OBSMODE, where *xxxx* is the central wavelength specified on the Phase II proposal.

Figure 3.4: FR418N and FR533N Wavelength Mapping.

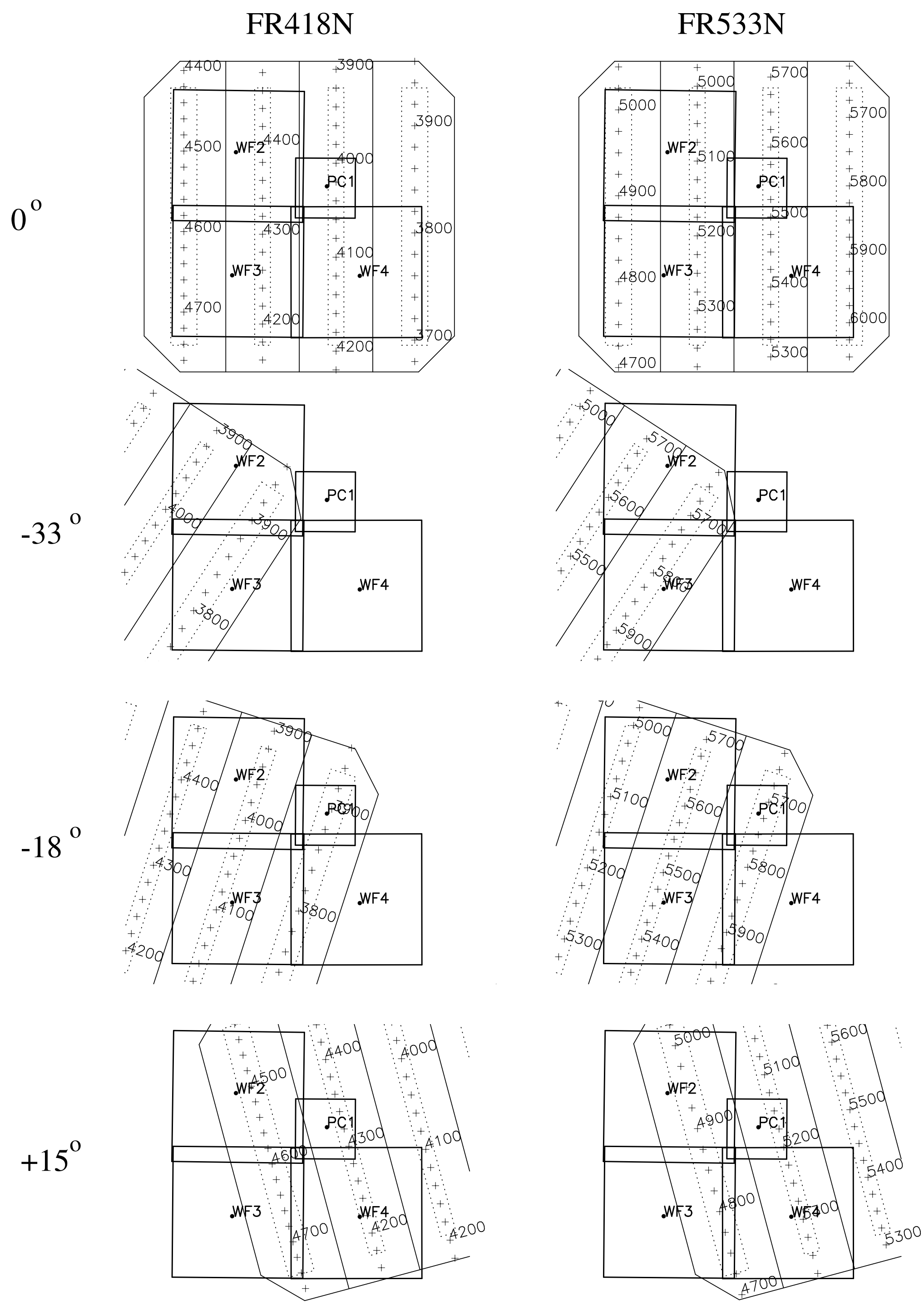

Figure 3.5: FR680N and FR868N Wavelength Mapping.

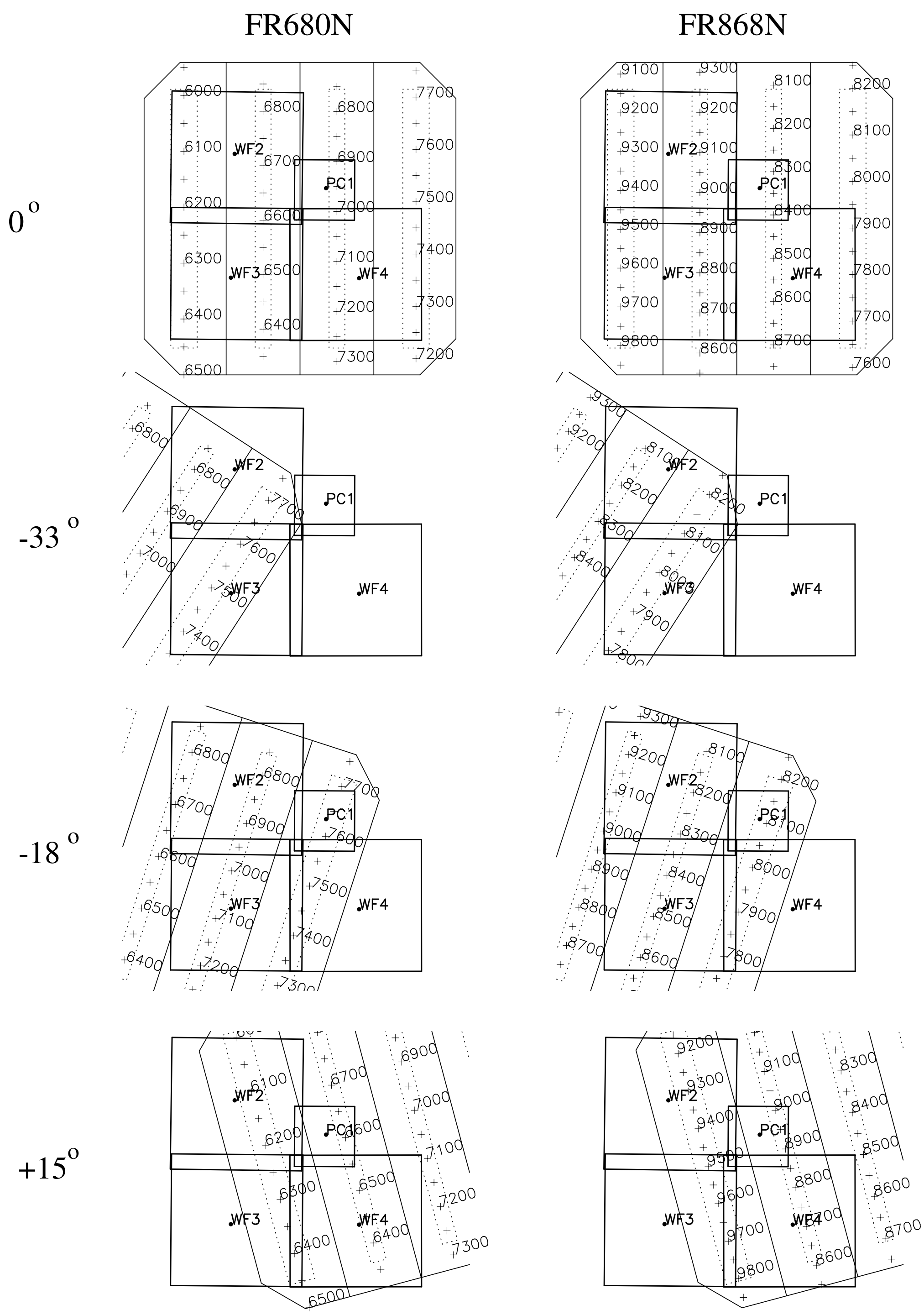

Table 3.7: Aperture Locations and Wavelengths for Ramp Filters.

Start (Å)	End (Å)	Filter	CCD / Aperture	x1 (pix)	y1 (pix)	x2 (pix)	y2 (pix)
3710	3800	FR418N	WF4-FIX	750	736.8	161 .5	737.7
3800	3878	FR418N33	WF3-FIX	669.5	559.2	395.1	128.9
3881	3907	FR418N18	PC1-FIX	402.3	225	515.4	579.5
3907	3929	FR418N33	WF2-FIX	128.4	286.7	250.1	209.9
3929	4008	FR418N18	WF2-FIX	562.7	233	130.1	367.1
4008	4038	FR418N	PC1-FIX	541.3	632.7	543.3	256.5
4038	4100	FR418N18	WF3-FIX	425.3	130.8	532 4	469.9
4100	4177	FR418N	WF4-FIX	309	276.2	750.3	275.5
4186	4210	FR418P15	WF4-FIX	596.5	515.9	469.4	482.1
4210	4308	FR418N	WF3-FIX	248.2	665.9	252.7	128.5
4308	4337	FR418P15	PC1-FIX	690.2	264.6	598.4	599.9
4337	4446	FR418N	WF2-FIX	127.9	247.6	725.4	255.7
4446	4550	FR418N	WF2-FIX	691.7	716.2	180.6	709.2
4550	4571	FR418P15	WF2-FIX	230	253.8	130.7	225.8
4593	4720	FR418N	WF3-FIX	713.7	125.6	708.5	749.9
4746	4863	FR533N	WF3-FIX	689.3	748.9	694.4	135.5
4884	4900	FR533P15	WF2-FIX	128.3	205.1	209	227.9
4900	5013	FR533N	WF2-FIX	153.6	689.6	745.9	697.7
5013	5020	FR533N18	WF2-FIX	693.4	642.4	662.9	651.8
5020	5153	FR533N	WF2-FIX	737.3	236.6	130	228.4
5153	5176	FR533P15	PC1-FIX	637.9	614.9	698.6	393.3
5188	5310	FR533N	WF3-FIX	233.5	127.4	228.8	684.7
5310	5335	FR533P15	WF4-FIX	482.8	505.5	593.1	534.9
5339	5450	FR533N	WF4-FIX	750.9	294.7	277.2	295.5
5450	5528	FR533N18	WF3-FIX	504.4	445.3	404.1	127.6
5528	5566	FR533N	PC1-FIX	585.3	277.5	583.4	632.3
5566	5671	FR533N18	WF2-FIX	124.1	348.8	552.3	216.1
5671	5700	FR533N33	WF2-FIX	224.8	203.2	122.3	267.7
5700	5741	FR533N18	PC1-FIX	558.8	577	444.9	220.1
5743	5910	FR533N33	WF3-FIX	370.8	126.5	745.9	714.9
5910	6007	FR533N	WF4-FIX	333.8	747.6	738.8	746.9
6007	6192	FR680N	WF2-FIX	750.3	706.9	122.9	698.4
6192	6208	FR680P15	WF2-FIX	177.1	228.4	124.9	213.6
6238	6409	FR680N	WF3-FIX	703.6	128.1	698.8	708.2
6409	6584	FR680N	WF3-FIX	237.8	705.6	242.6	127
6590	6631	FR680P15	PC1-FIX	699.1	315.3	620.9	601.2
6631	6800	FR680N	WF2-FIX	125.9	237.5	684.5	245.1
6800	6921	FR680N18	WF2-FIX	480.1	248	129.9	356.6
6921	6976	FR680N	PC1-FIX	563.3	639.2	565.3	274.6
6976	7061	FR680N18	WF3-FIX	413.2	126	490.8	371.7
7061	7241	FR680N	WF4-FIX	203	286.4	748.3	285.6
7251	7420	FR680N	WF4-FIX	749.6	743.5	213.3	744.3
7420	7600	FR680N33	WF3-FIX	688.9	608.4	381.6	126.4
7605	7658	FR680N18	PC1-FIX	427	230	538.9	580.6
7658	7690	FR680N33	WF2-FIX	126.2	276.1	212.1	222
7690	7830	FR868N	WF4-FIX	711.5	751.3	316.5	751.9
7830	8072	FR868N33	WF3-FIX	728.2	705.8	360.9	129.7
8077	8140	FR868N18	PC1-FIX	471.5	231	589.7	601.5
8140	8300	FR868N18	WF2-FIX	527.6	213.2	126.2	337.6
8300	8362	FR868N	PC1-FIX	605.4	644.1	607.3	287.9
8362	8460	FR868N18	WF3-FIX	393.1	126.1	470.6	371.7
8460	8661	FR868N	WF4-FIX	196.9	305.7	724.7	304.9
8661	8910	FR868N	WF3-FIX	218.3	731.6	223.4	125.3
8945	8980	FR868P15	PC1-FIX	701.1	467.5	651.9	647.3
8980	9200	FR868N	WF2-FIX	142.7	218.5	678.2	225.8
9200	9415	FR868N	WF2-FIX	668.4	686.5	162.2	679.6
9415	9456	FR868P15	WF2-FIX	219.9	220.5	127	194.2
9501	9762	FR868N	WF3-FIX	684.3	135.4	679.2	750.2

Table 3.8: Vignetted Wavelengths for Ramp Filters. The right column gives the maximum throughput reduction (in %) for these settings where the target must be placed away from the optimal location on the filter glass. "FOV" denotes settings where transmission is optimal, but the usable field-of-view is reduced below 10″ to the indicated diameter (in arcseconds).

Start (Å)	End (Å)	Filter	CCD / Aperture	x1 (pix)	y1 (pix)	x2 (pix)	y2 (pix)	Max % Light Loss
3878	3881	FR418N18	PC1-FIX	402.3	225.0	402.3	225.0	2
4177	4182	FR418N	WF4-FIX	750.3	275.5	750.3	275.5	3
4182	4186	FR418P15	WF4-FIX	596.5	515.9	596.5	515.9	2
4571	4582	FR418P15	WF2-FIX	130.7	225.8	130.7	225.8	13
4582	4593	FR418N	WF3-FIX	713.7	125.6	713.7	125.6	13
4720	4733	FR418N	WF3-FIX	708.5	749.9	708.5	749.9	14
4733	4746	FR533N	WF3-FIX	689.3	748.9	689.3	748.9	14
4863	4873	FR533N	WF3-FIX	694.4	135.5	694.4	135.5	8
4873	4884	FR533P15	WF2-FIX	128.3	205.1	128.3	205.1	8
5176	5183	FR533P15	PC1-FIX	698.6	393.3	698.6	325.9	FOV~9"
5183	5188	FR533N	WF3-FIX	233.5	127.4	233.5	127.4	2
5335	5337	FR533P15	WF4-FIX	593.1	534.9	593.1	534.9	1
5337	5339	FR533N	WF4-FIX	750.9	294.7	750.9	294.7	1
5741	5743	FR533N33	WF3-FIX	370.8	126.5	370.8	126.5	1
6208	6221	FR680P15	WF2-FIX	124.9	213.6	124.9	213.6	8
6221	6238	FR680N	WF3-FIX	703.6	128.1	703.6	128.1	11
6584	6587	FR680N	WF3-FIX	242.6	127.0	242.6	127.0	1
6587	6590	FR680P15	PC1-FIX	699.1	294.3	699.1	315.3	FOV~9"
7241	7246	FR680N	WF4-FIX	748.3	285.6	748.3	285.6	2
7246	7251	FR680N	WF4-FIX	749.6	743.5	749.6	743.5	2
7600	7602	FR680N33	WF3-FIX	381.6	126.4	381.6	126.4	1
7602	7605	FR680N18	PC1-FIX	427.0	230.0	427.0	230.0	1
8072	8074	FR868N33	WF3-FIX	360.9	129.7	360.9	129.7	1
8074	8077	FR868N18	PC1-FIX	471.5	231.0	471.5	231.0	1
8910	8920	FR868N	WF3-FIX	223.4	125.3	223.4	125.3	2
8920	8945	FR868P15	PC1-FIX	701.1	339.1	701.1	467.5	FOV~7"
9456	9478	FR868P15	WF2-FIX	127.0	194.2	127.0	194.2	13
9478	9501	FR868N	WF3-FIX	684.3	135.4	684.3	135.4	13

3.4 Redshifted [OII] Quad Filters

The redshifted [OII] quad filter was designed to map onto a four-faceted WFC configuration. A partial SOFA wheel rotation of -33° is required to move filter quadrant 1 (3763Å) into WF2 and WF3, with some vignetting of both camera fields. The projections of the redshifted [OII] filter settings FQUVN and FQUVN33 onto the field-of-view are essentially identical to those of the POLQ and POLQN33 filters, respectively (Figure 3.6). The vignetted regions are similar, and the location of aperture FQUVN33 is identical to that of POLQN33.

The nominal and rotated filter wheel positions for the redshifted [OII] quad filter are each associated with different filter names. This allows pipeline calibration and database retrievals to proceed smoothly. The filter names are summarized in Table 3.9.

The required central wavelength is selected by filter name and aperture location. Filter element FQUVN (Filter Quad UltraViolet Narrow) has three possible apertures, each of which is nominally centered in one of the three WF channels and associated with a unique central wavelength. The filter element FQUVN33 corresponds to a single central wavelength. In addition to the filter name and aperture, a central wavelength is also requested in the proposal instructions in order to provide a consistency check. Aperture names are discussed further in section 3.9, "Apertures", on page 60.

Table 3.9: Redshifted [OII] Quad Filter Elements.

Filter Name	Aperture Name	FOV Location	Quad	Mean Wavelength (Å)	Effective Width (Å)	Comments
FQUVN	WF2	WF2	D	3992	64	Nominal filter wheel position
FQUVN	WF3	WF3	C	3913	59	Nominal filter wheel position
FQUVN	WF4	WF4	B	3830	57	Nominal filter wheel position
FQUVN33	FQUVN33	WF2	A	3765	73	Filter rotated -33˚

3.5 Polarizer Quad Filter

The polarizer quads were also designed to map onto a four-faceted WFC configuration and, consequently, also require a partial filter rotation of -33˚ to move the filter quadrant 1 (nominal polarization angle 135˚) into WFCs 2 and 3, with some vignetting of both camera fields. Several additional partial rotations have been added to allow observations with different polarization angles on the same CCD.

The polarizer quad may be used in several ways: by observing the target with each camera, by observing the target with the same camera using different partial rotations of the polarizer quad, or by observing the target with the same camera using different roll angles of the spacecraft. The first method has the drawback that calibration is complicated by uncertainties in the relative photometric calibration between cameras, while the second method uses the same camera but has non-optimal polarization angles and limited fields of view. The third method may present scheduling difficulties due to constraints on the spacecraft roll angle, and the need to rotate undersampled images. (See Biretta and Sparks 1995, "WFPC2 Polarization Observations: Strategies, Apertures, and Calibration Plans," WFPC2 Instrument Science Report 95-01.)

The polarizer is designed for problems where large polarization angles are observed, and is not suitable for problems requiring precision of order 3% or better. The required polarization angle is selected by filter name and aperture location. The transmission of the quad polarizer is shown in Figure 3.7. The

Table 3.10: Polarizer Quad Filter. Polarization angle 0˚ lies along +X direction in Figure 3.11

Filter Name	Aperture Name	FOV Location	Polarization Angle	Comments
POLQ	PC1	PC1	135˚	Nominal filter wheel position
POLQ	WF2	WF2	0˚	Nominal filter wheel position
POLQ	WF3	WF3	45˚	Nominal filter wheel position
POLQ	WF4	WF4	90˚	Nominal filter wheel position
POLQN33	POLQN33	WF2	102˚	Filter wheel rotated -33˚
POLQP15	POLQP15P	PC	15˚	Filter wheel rotated +15˚
POLQP15	POLQP15W	WF2	15˚	Filter wheel rotated +15˚
POLQN18	POLQN18	WF2	117˚	Filter wheel rotated -18˚

polarizer is afocal and must therefore usually be used with another filter which will largely define the shape of the passband.

Figure 3.6: Polarizer Quads. The schematics show the filter projected onto the field-of-view for all rotated positions. Apertures are marked. Dashed lines indicate the central region of each quad which is free of vignetting and cross-talk. Greyscale images are VISFLATs of the polarizer with F555W.

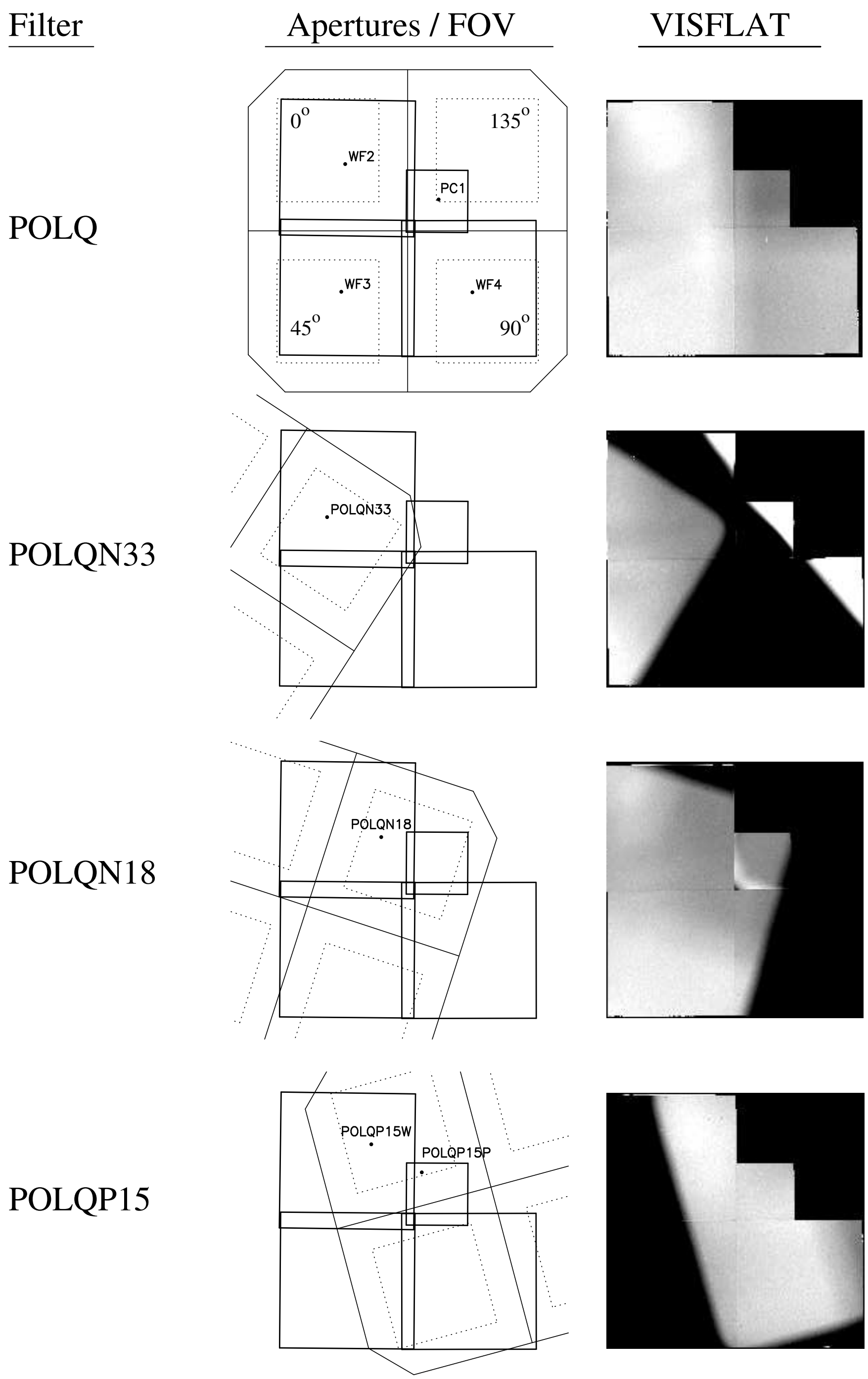

Figure 3.7: Polarizer Transmission for light polarized perpendicular (dotted curve) and parallel (solid curve) to the filter polarization direction.

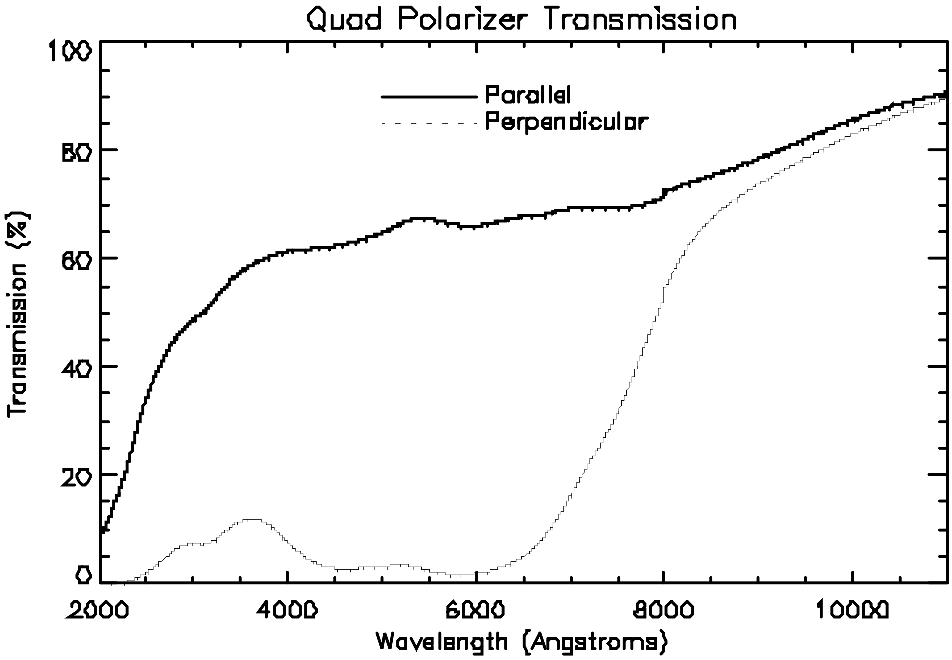

3.6 Methane Quad Filter

The methane band quad filter, known as the jewel-quad, was designed for a four-faceted WF/PC configuration to permit imaging with both four WFC CCDs and four PC CCDs. WFC imaging is recovered for the first quadrant element of the filter (6193Å) by a partial SOFA wheel rotation of -33° which moves quadrant 1 into WF2 and WF3 with some vignetting of both camera fields. PC imaging with all four elements of the methane band jewel-quad cannot be recovered, but partial SOFA wheel rotations of -15° and +15° are implemented to recover two of the four methane band filters (8929Å and 6193Å). The +15° rotation of the filter wheel, however, results in some vignetting of PC1's field-of-view. The filter projections associated with the methane band jewel-quad are shown in Figure 3.8. Each of the four filter wheel positions are associated with unique filter names, as summarized in Table 3.11 on page 54.

The required central wavelength is selected by filter name and aperture location. Filter element FQCH4N (Filter Quad Methane Narrow) has three possible apertures, each of which is located in one of the three WF channels and associated with a unique central wavelength, while FQCH4N33 is associated with one possible central wavelength. FQCH4N15 and FQCH4P15 are both associated with one central wavelength for PC1 observations. In addition to the filter name and aperture, a central wavelength is also requested in the proposal instructions in order to provide a consistency check.

Table 3.11: Methane Band Quad Filter. The filter and aperture names should be specified on the Phase II proposal as shown here.

Filter Name	Aperture Name	FOV Location	Quad	Mean Wavelength (Å)	Effective Width (Å)	Comments
FQCH4N	FQCH4W2	WF2	A	5433	38	Nominal filter position
FQCH4N	FQCH4W3	WF3	D	8929	64	Nominal filter position
FQCH4N	FQCH4W4	WF4	C	7274	51	Nominal filter position
FQCH4N33	FQCH4N33	WF2/WF3	B	6193	44	Filter rotated -33˚
FQCH4N15	FQCH4N15	PC1	B	6193	44	Filter rotated -15˚
FQCH4P15	FQCH4P15	PC1	D	8929	64	Filter rotated +15˚

3.7 Wood's Filters

WFPC2 features two solar-blind Wood's filters, for FUV (<2000Å) imaging. It was shown by Wood in the 1930s (Physical Optics, 1934, R. W. Wood) that thin layers of alkali metals transmit FUV wavelengths while providing very efficient long wavelength blocking due to the plasma frequency of the free electrons. Wood's filters have been built for WFPC2 at JPL using thin (5000Å) layers of sodium sandwiched between two MgF_2 substrates. These Wood's filters have a broad bandpass from 1200Å to 2100Å with visible-light transmission lower than 10^{-8}. The best conventional UV filters exhibit visible-light transmission of 10^{-3} to 10^{-4}. Many astronomical objects emit 10^4 to 10^7 visible photons for every FUV photon. In such cases, a Wood's filter (or "solar blind" detector as on STIS) is essential for FUV imaging so that the visible light leak does not dominate the observation. The main problem experienced with Wood's filters is long term instability. Sodium is a very reactive metal, and attempts to passivate the sodium layer have met with limited success. It is possible that as the Wood's filters age pinholes will form which transmit visible light. This transmitted light will appear as an increase in the background level at the focal plane. No indications of any degradation on-orbit have been observed.

Figure 3.8: Methane Quad Filter. The mapping to the focal plane for nominal and rotated (-33°, -15°, and +15°) SOFA positions is shown. Dashed lines indicate the limits of the unvignetted field-of-view on each quad.

Filter	Apertures / FOV
FQCH4N	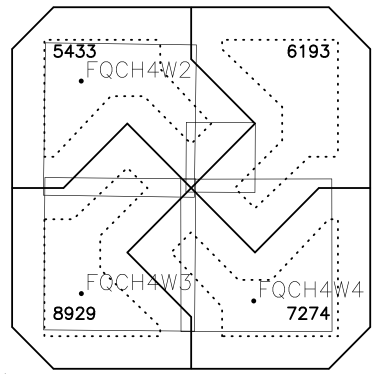
FQCH4N33	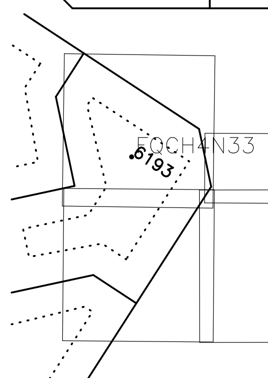
FQCH4N15	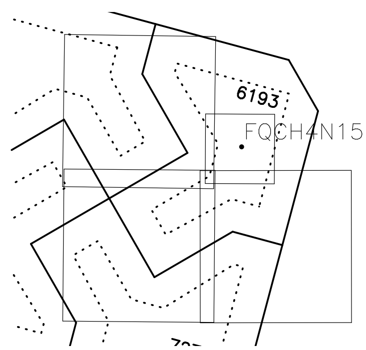
FQCH4P15	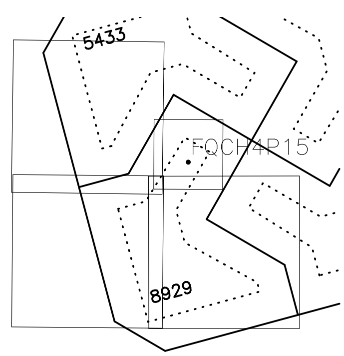

Figure 3.9: Wood's Filters. Greyscale flat field images show the field-of-view available with the two Wood's filter options F160BW and F160BN15.

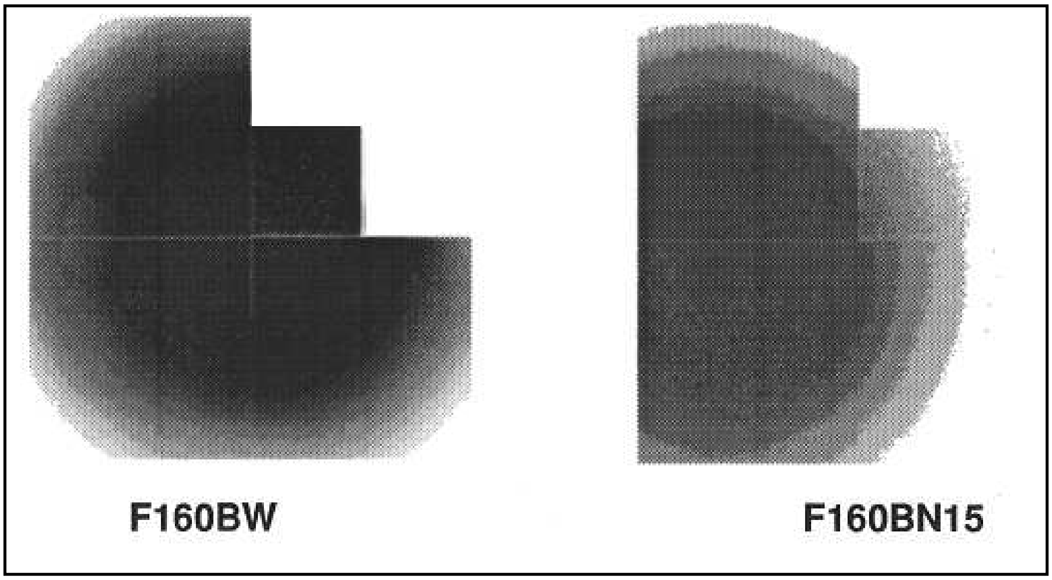

The Wood's filters can be used as a broadband filter, or in combination with the CaF_2 long-pass filter to suppress geocoronal emission, or, crossed with one of the other UV filters, such as the suprasil blocker F165LP, to define a solar-blind UV photometric system. As discussed at the beginning of this chapter, the image will be out of focus in the last case. WFPC2's Wood's filters are circular with a clear aperture of 41 mm. Two similar Wood's filters (F160AW and F160BW) were mounted in SOFA wheel 1 to provide some redundancy. In Thermal Vacuum testing F160AW showed evidence for pinholes, which cause excessive red leak in some parts of its field. Therefore the preferred filter for far UV imaging with minimal red leak in WFPC2 is F160BW.

In the nominal filter wheel position PC1 has a clear field-of-view but, there is significant vignetting in all three WFCs. A partial filter wheel rotation of -15° produces a larger field-of-view in WF3, although some vignetting remains. The options are illustrated in Figure 3.9. The imaging performance of the Wood's filters is continually monitored for signs of aging such as visible light leaks. Additional partial rotations could be implemented in the future, to position an unaffected region of the filter into a WF or PC1, if necessary. The unvignetted filter projections associated with the two planned filter positions are shown schematically in Figure 3.9. Each filter position is associated with a unique name as summarized in Table 3.12.

The filter name must be selected on the basis of whether a PC or WF3 observation is required.

Table 3.12: Wood's Filters. The filter and aperture names should be specified on the Phase II proposal as shown below.

Filter Name	Aperture Name	FOV Location	Mean Wavelength (Å)	Effective Width (Å)	Comments
F160BW	PC1	PC1	1600	900	Nominal filter position
F160BN15	F160BN15	WF3	1600	900	Filter rotated -15°

3.8 Red Leaks in UV Filters

The "red leaks" in the UV filters are shown in Figure 3.10 for F122M, F160BW (the new Wood's filter), F170W, F185W F218W F255W, F300W, and F336W. The presence of significant red leaks in the UV filters, together with the much greater sensitivity and wavelength coverage in the red part of the spectrum, makes calibration of UV observations difficult. Table 3.13 shows red leak estimates as a percentage of the total detected flux from de-reddened stellar sources, ordered by spectral type. In each column, the red leak is defined as the percentage of the detected flux longward of the cutoff wavelength in the second row. In the presence of interstellar reddening, the red leaks will be larger. Note that the SYNPHOT synthetic photometry package can be used to estimate the counts contributed by red leak for various particular situations, and for filters other than those plotted below.

There is significant variation of the UV throughput due to build-up of molecular contaminants on the CCD windows, and decontamination procedures used to remove this contamination. See "Time Dependence of UV Response" on page 137.

Figure 3.10: UV Filter Red Leaks. Includes the on-orbit measurements of system response.

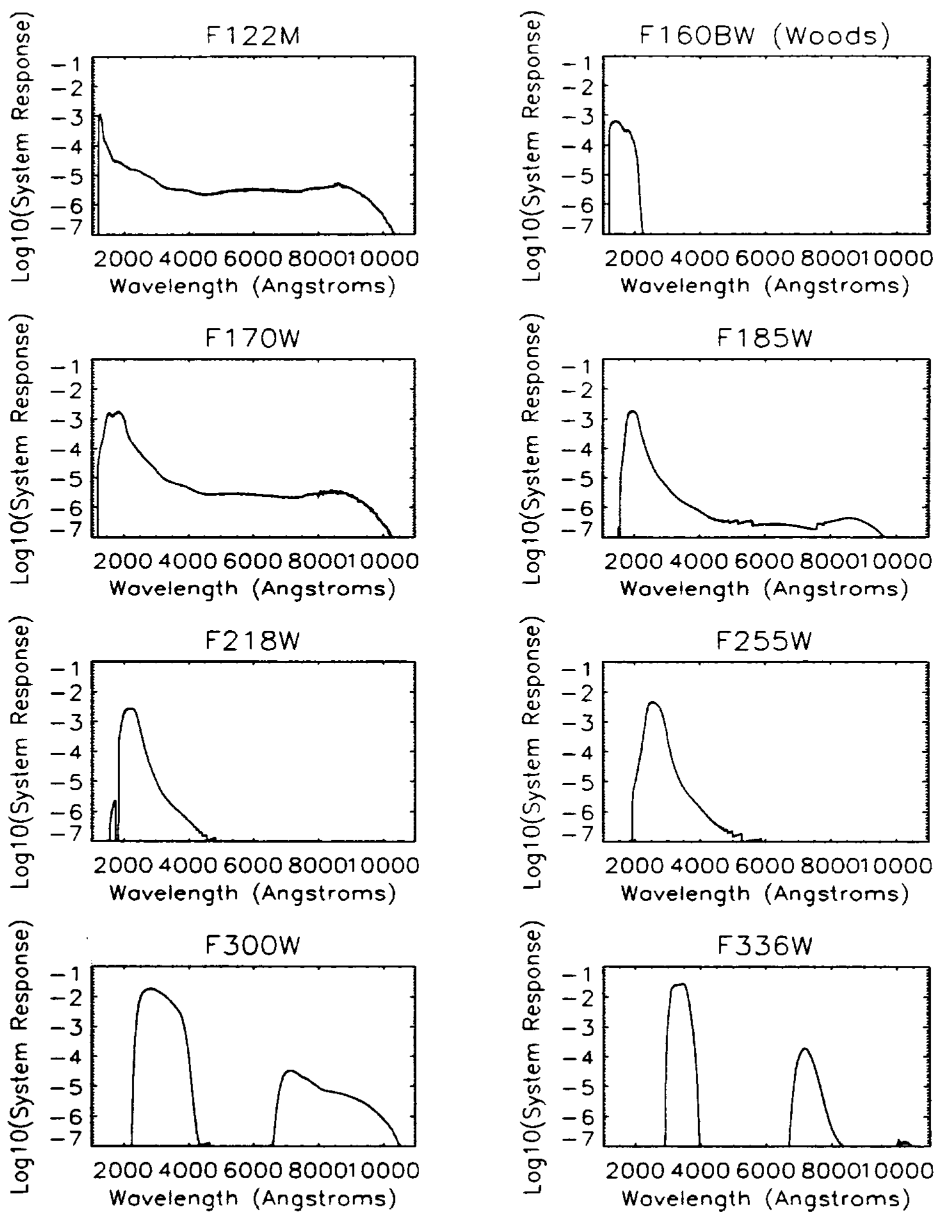

Table 3.13: Red Leak in UV Filters. A synthetic photometry calculation with de-reddened BPGS stellar spectra and system response from on-orbit data.

Filter		F122M	F160BW	F170W	F185W	F218W	F255W	F300W	F336W	F122M	F160B	F170W	F185W	F218W	F255W	F300W	F336W
Filter Central λ (nm)		122	160	170	185	218	255	300	336	122	W160	170	185	218	255	300	336
Cutoff λ (nm)		140	240	260	260	280	310	400	400	380	380	380	380	380	380	380	380
9SGR	O5	16.9		0.7	0.4	0.2	0.3		0.1	0.3		0.1				0.5	0.1
9 SGE	O8F	16.9		0.7	0.4	0.2	0.3		0.1	0.3		0.1				0.5	0.1
HR8D23	O6	21.8		1.0	0.5	0.3	0.4		0.1	0.6		0.1				0.6	0.1
-1935	B1V	20.1		0.8	0.4	0.3	0.4		0.1	0.6		0.1				0.6	0.2
60CYG	B1V	20.1		0.8	0.4	0.3	0.4		0.1	0.6		0.1				0.6	0.2
102 HER	B2V	22.5		1.2	0.6	0.4	0.4	0.1	0.1	1.1		0.2	0.1			0.8	0.2
ETAHYA	B3V	22.7		1.2	0.6	0.4	0.5	0.1	0.1	1.3		0.3	0.1			0.9	0.2
IOTA HER	B3V	22.7		1.2	0.6	0.4	0.5	0.1	0.2	1.3		0.3	0.1			0.9	0.2
HR 7899	B4V	22.7		1.2	0.6	0.4	0.5	0.1	0.2	1.4		0.3	0.1			0.9	0.2
38OPH	A1V	30.0		1.6	0.7	0.5	0.5	0.1	0.2	2.9		0.5	0.1			1.1	0.3
HR7174	B6V	30.7		1.8	0.8	0.5	0.5	0.1	0.3	3.8		0.7	0.2		0.1	1.3	0.4
9 VUL	B7V	30.8		1.8	0.8	0.5	0.5	0.1	0.3	3.9		0.7	0.2		0.1	1.4	0.4
HD 189689	B9V	41.1		2.4	0.9	0.5	0.6	0.2	0.3	7.4		1.0	0.2		0.1	1.6	0.4
THETA VIR	A0V	59.6		4.0	1.2	0.6	0.8	0.3	0.6	20.3		2.2	0.4	0.1	0.1	2.5	0.7
NUCAP	B9V	58.6		3.7	1.2	0.6	0.8	0.3	0.5	18.3		2.0	0.4	0.1	0.1	2.2	0.6
HR6169	A2V	59.5		4.0	1.2	0.6	0.8	0.3	0.6	20.1		2.2	0.4	0.1	0.1	2.3	0.7
HD140849A	A1V	73.7		3.8	1.1	0.6	0.7	0.3	0.5	23.7		2.0	0.4	0.1	0.1	2.0	0.6
69HER	A2V	59.5		3.9	1.2	0.6	0.8	0.3	0.6	20.0		2.2	0.4	0.1	0.1	2.2	0.7
HD140849B	A3V	89.0		6.5	1.5	0.8	1.0	0.4	0.6	44.0		3.9	0.6	0.1	0.2	2.4	0.7
58AQL	A0V	75.5		4.3	1.3	0.6	0.8	0.3	0.7	28.6		2.5	0.5	0.1	0.1	2.7	0.8
78HER	B9V	75.0		4.2	1.2	0.6	0.7	0.3	0.7	27.5		2.4	0.5	0.1	0.1	2.4	0.8
HR6570	A7V	89.7		7.0	1.6	0.8	1.0	0.4	0.7	47.6		4.4	0.7	0.1	0.2	2.6	0.9
HD187754	A2V	97.9		11.0	2.1	0.9	1.2	0.5	0.9	64.4		7.4	1.0	0.2	0.2	3.2	1.1
THETA1SER	A5V	97.7		9.8	1.9	0.9	1.1	0.4	0.8	60.3		6.2	0.8	0.1	0.2	2.6	0.9
PRAESEPE 276		99.7		12.1	2.2	1.0	1.2	0.5	0.9	67.5		8.1	1.1	0.2	0.2	2.9	1.0
PRAESEPE114		99.7		11.6	2.2	1.0	1.2	0.5	0.9	66.0		7.6	1.0	0.2	0.2	2.7	1.0
PRAESEPE154		100.0		17.0	3.0	1.1	1.3	0.5	0.9	71.9		11.4	1.4	0.2	0.2	2.8	1.0
HD140192	A5V	100.0		17.4	3.0	1.1	1.3	0.6	0.9	72.7		11.7	1.5	0.2	0.2	2.9	1.1
PRAESEPE226		100.0		17.2	3.0	1.1	1.3	0.6	1.0	72.7		11.6	1.4	0.2	0.2	2.7	1.1
PRAESEPE37		100.0		38.8	7.7	2.0	1.7	0.6	1.0	80.8		27.0	3.9	0.3	0.3	2.8	1.1
HD191177	F4V	100.0		64.9	17.6	3.0	2.3	0.8	1.1	86.1		48.4	10.1	0.6	0.5	3.6	1.3
PRAESEPE332		100.0		62.4	16.3	2.9	2.2	0.7	1.0	84.6		44.9	8.8	0.5	0.4	2.9	1.1
BD+293891	F6V	100.0		67.4	19.4	3.7	2.5	0.8	1.1	86.4		49.8	11.0	0.7	0.4	3.1	1.2
PRAESEPE222		100.0		50.7	11.4	2.8	2.2	0.8	1.1	84.7		36.8	6.2	0.5	0.4	2.8	1.2
HD35246	F8V	100.0		52.1	11.8	2.9	2.2	0.8	1.3	85.8		38.6	6.6	0.5	0.4	2.8	1.4
BD+263780	G0V	100.0		52.4	11.9	2.9	2.2	0.9	1.3	86.0		38.9	6.7	0.5	0.4	2.8	1.4
HD 148816	F9V	100.0		51.1	11.5	2.8	2.2	0.8	1.2	85.0		37.2	6.3	0.5	0.3	2.8	1.3
HD155675	F8V	100.0		69.0	20.5	4.7	3.4	1.0	1.3	88.7		53.3	12.4	0.9	0.6	3.3	1.4
PRAESEPE 418		100.0		70.2	21.1	4.8	3.5	1.0	1.4	89.4		55.0	13.2	1.0	0.6	3.2	1.5
HYAD 1		100.0		71.4	21.9	4.8	3.5	1.1	1.5	90.0		56.8	14.1	1.0	0.6	3.4	1.6
HD 122693	F8V	100.0		71.6	22.1	4.9	3.5	1.1	1.6	90.1		57.1	14.2	1.1	0.6	3.5	1.7
HD 154417	F8V	100.0		70.6	21.4	4.8	3.5	1.1	1.4	89.5		55.5	13.4	1.0	0.6	3.2	1.5
HYAD 2		100.0		89.2	46.7	7.9	3.4	1.2	1.6	91.2		71.6	30.3	1.7	0.6	3.3	1.7
HD 227547	G5V	100.0		89.5	47.2	8.0	3.4	1.2	1.7	91.4		72.0	30.7	1.7	0.6	3.3	1.8
HD 154760	G2V	100.0		89.3	46.8	7.9	3.4	1.2	1.6	91.3		71.6	30.3	1.7	0.6	3.3	1.7
HD 140605	G2V	100.0		89.9	48.2	8.1	3.5	1.3	1.8	91.8		73.2	32.0	1.8	0.7	3.4	1.9
HYAD 15		100.0		90.1	48.5	8.0	3.5	1.3	1.8	92.1		73.7	32.5	1.8	0.7	3.4	1.9
HD 139777A	K0V	100.0		89.8	47.7	8.0	3.4	1.3	1.8	91.7		72.8	31.5	1.7	0.6	3.5	1.9
HD 136274	G8V	100.0		91.4	51.6	8.3	3.5	1.7	2.3	93.4		77.1	36.6	2.0	0.7	3.6	2.4
HYAD26		100.0		91.6	52.3	8.3	3.6	1.7	2.3	93.5		77.6	37.3	2.1	0.7	3.6	2.4
HD 150205	G5V	100.0		91.7	52.3	8.4	3.6	1.7	2.4	93.5		77.6	37.4	2.1	0.8	3.8	2.4
HYAD 21		100.0		92.8	55.7	8.6	3.7	2.1	2.8	94.6		80.7	41.8	2.4	0.8	3.9	2.9
+02 3001	G8V	100.0		93.0	56.1	8.6	3.6	2.2	3.1	94.8		81.1	42.3	2.4	0.8	4.3	3.2
HD190571	G8V	100.0	0.3	99.5	95.2	40.0	11.3	3.4	3.6	96.7	0.1	91.4	80.4	16.0	3.0	6.1	3.7
HYAD183		100.0	0.3	99.6	96.0	41.6	11.7	4.3	4.6	97.5	0.1	93.1	83.8	18.3	3.4	6.7	4.7
HD140470	K3V	100.0	0.3	99.6	96.2	42.2	11.9	4.5	4.8	97.5	0.1	93.3	84.4	19.0	3.5	7.0	4.9
HD154712	K4V	100.0	0.2	99.7	95.7	45.7	15.8	6.6	6.7	98.3	0.1	95.3	87.4	24.6	5.4	9.4	6.8
HYAD185		100.0	0.2	99.7	96.7	50.0	15.7	8.0	7.9	98.6	0.1	96.0	89.5	28.6	5.5	10.6	8.0
+382457	K8V	100.0	0.2	99.7	96.6	48.6	16.5	8.8	9.1	98.7	0.1	96.4	90.1	28.7	6.3	11.5	9.1
HYAD173		100.0	0.1	99.5	93.8	32.0	8.5	11.8	12.8	99.0		96.9	88.7	19.8	3.8	14.3	12.9
GL40	M0V	100.0	0.1	99.6	94.9	34.5	8.8	14.5	15.4	99.2		97.5	90.7	22.8	4.2	17.4	15.5
HYAD 189		100.0	0.1	99.6	95.3	35.8	9.1	15.7	16.8	99.3		97.7	91.5	24.3	4.4	18.4	16.9
HD 151288	K7V	100.0	0.1	99.7	95.6	37.0	9.4	16.5	17.4	99.3		97.8	91.9	25.5	4.7	19.3	17.4
HD157881	K7V	100.0	0.1	99.7	95.6	36.6	9.2	16.7	17.6	99.3		97.8	91.9	25.2	4.5	19.4	17.7
HD1326d3	M0V	100.0	0.1	99.7	95.8	37.5	9.4	17.7	18.9	99.4		97.9	92.3	26.2	4.7	20.5	18.9
GL15A	M0V	100.0	0.1	99.8	97.7	48.6	11.5	27.3	26.7	99.6	0.1	98.8	95.6	38.8	6.7	30.4	26.8
GL49	M2V	100.0	0.1	99.8	97.3	45.8	10.7	25.5	25.0	99.6	0.1	98.7	95.1	35.9	6.0	28.7	25.1
GL1D9	M4V	100.0	0.1	99.9	98.2	54.5	12.5	34.1	32.2	99.7	0.1	99.1	96.7	46.1	7.9	37.2	32.3
GL15B	M6V	100.0	0.2	99.9	99.2	69.7	17.7	51.1	46.0	99.9	0.1	99.6	98.4	64.0	13.3	53.5	46.1
GL83.1	M8V	100.0	0.1	99.7	95.9	38.2	8.9	17.4	15.5	99.4		97.9	92.4	26.8	3.9	20.1	15.5
GL65	M5V	100.0	0.1	99.8	97.0	43.3	9.2	22.4	17.8	99.6		98.5	94.4	33.0	4.3	25.2	17.9

3.9 Apertures

The WFPC2 camera configuration and filter set require a substantial number of apertures for full utilization of its capabilities. All possible aperture and filter combinations are given in Table 3.14.

Each camera has an associated 'optimum' aperture close to the geometric center of its field-of-view (FOV). These positions have been adjusted to reflect CCD performance following SMOV and to allow for pyramid vignetting. The aperture designations are WF2, WF3, WF4, and PC1 for the individual cameras and WFALL for the three-WFC combination. WFALL is located close to the apex in WF3 (see Figure 3.11). Observers are expected to place small or unresolved targets on these apertures. Note that normally all four CCDs are read out even if a specific CCD is selected with an aperture. This is discussed in section 2.8, "CCD Orientation and Readout", on page 31.

In cases where the observer does not want to use the current 'optimum' centers, a complimentary set of apertures has been implemented specifically for this purpose. These locations remain fixed and correspond roughly to the geometric center of each camera's field-of-view. They are designated WF2-FIX, WF3-FIX, WF4-FIX, PC1-FIX, and WFALL-FIX. Observers are expected to place extended targets on these apertures.

An additional set of aperture names have been defined for use with the WFPC2 filters which require partial rotations. The characteristics and uses of these filters are discussed earlier in this Chapter. In the nominal filter position, the three WFC segments of the [OII], Methane and Polarizer quad filters can be selected with an aperture for each camera corresponding to the optimum or geometric camera centers. The partially rotated quad filters, which generally fall into more than one camera, have been assigned apertures in the camera which provides the largest clear aperture. The pixel coordinates of these apertures will be reviewed on a regular basis to reflect changes in CCD and filter cosmetics. There are no analogous fixed apertures for the partially rotated filter configurations. The aperture name is generally the same as the (rotated) filter name. For the Wood's filters, the nominal filter position is used for the PC1 FOV only, while the rotated filter position is used for WFC observations. The linear ramp filters are unique because the ultimate location of the target will be determined from the central wavelength specified and so an aperture name is not required.

Occasionally the V2-V3 coordinates of the WFPC2 apertures are updated to correct slow drifts of the HST focal plane relative to the spacecraft (V1, V2, V3) system. Table 3.15 shows this history. The previous V2-V3 coordinates for any aperture can be derived by setting ($V2_2$,$V3_2$) to the values in Table 3.14, and then computing the earlier coordinates.

Table 3.14: Aperture Definitions. The pixel coordinate system uses pixel numbers (row, column) for the CCD in use. See Figure 3.11: on page 62 or Figure 1.1: on page 2 for the definition of the V2-V3 coordinate system.

Aperture Name	Filter Name	CCD	Location	CCD Pixel X	CCD Pixel Y	Coordinates[a] V2	Coordinates[a] V3
PC1		PC	Optimum center PC	420	424.5	2.160	-30.490
WF2		WF2	Optimum center WF2	423.5	414	-51.530	-5.920
WF3		WF3	Optimum center WF3	436[b]	424.5[b]	-0.150	48.470
WF4		WF4	Optimum center WF4	423	421	54.830	-6.320
WFALL		WF3	Optimum near apex	133[c]	149[c]	2.020	7.920
PC1-FIX		PC	Fixed center PC	420	424.5	1.810	-30.900
WF2-FIX		WF2	Fixed center WF2	423.5	414	-51.530	-5.920
WF3-FIX		WF3	Fixed center WF3	416.5	424.5	1.230	47.100
WF4-FIX		WF4	Fixed center WF4	423	421	54.830	-6.320
WFALL-FIX		WF3	Fixed near apex	133[c]	149[c]	2.020	7.920
FQUVN33	FQUVN33	WF2	Optimum for FOV	292	520	-49.924	10.802
POLQN33	POLQN33	WF2	Optimum for FOV	292	520	-49.924	10.802
POLQN18	POLQN18	WF2	Optimum for FOV	380[d]	200[d]	-33.280	-17.717
POLQP15P	POLQP15	PC	Optimum for FOV	200	680	-13.057	-31.643
POLQP15W	POLQP15	WF2	Optimum for FOV	500	260	-45.892	-22.069
FQCH4NW2	FQCH4N	WF2	Optimum for FOV	602	608	-77.669	-5.102
FQCH4NW3	FQCH4N	WF3	Optimum for FOV	602	608	0.928	72.995
FQCH4NW4	FQCH4N	WF4	Optimum for FOV	640	386	67.687	11.323
FQCH4N33	FQCH4N33	WF2	Optimum for FOV	264	436	-41.997	6.950
FQCH4N15	FQCH4N15	PC	Optimum for FOV	420	424.5	2.164	-30.494
FQCH4P15	FQCH4P15	PC	Optimum for FOV	400	312	5.129	-26.221
F160BN15	F160BN15	WF3	Optimum for FOV	436	424.5	-0.153	48.470

a. V2-V3 coordinates in effect after 1996 day 127 (May 6). CCD pixel positions unchanged.
b. CCD pixel position in effect after 1994 day 101 (April 11).
c. WFALL and WFALL-FIX “meta-chip” coordinates are (903,904).
d. CCD pixel position in effect after 1995 day 86 (March 27).

Table 3.15: Updates to (V2,V3) Positions of WFPC2 Apertures.

Date in Effect	V2	V3	Rotation
1994 day 101 - 1996 day 105	$V2_0$	$V3_0$	PA_0
1996 day 105 - 1996 day 127	$V2_1 = V2_0 - 0.12''$	$V3_1 = V3_0 + 0.11''$	$PA_1 = PA_0 + 0.14^{\circ}$
>1996 day 127	$V2_2 = V2_0 + 0.46''$	$V3_2 = V3_0 + 0.39''$	$PA_2 = PA_0 + 0.14^{\circ}$

Figure 3.11: Precise CCD Alignments and Primary Aperture Locations. "FIX" apertures are in the same locations, unless otherwise indicated. Dashed lines show vignetted region along CCD boundaries. Short lines and "X"s in outer corners indicate directions of CCD bloom and OTA diffraction spikes, respectively. Origin of the (V2, V3) system is at the origin of the plot axes, with V2, V3, and U3 exactly along diagonal lines as marked. (V2,V3) system is post-1996 day 127. CCDs have pixel (1,1) located where the four CCDs overlap.